Polarforschung 54 (2): 85—93, 1984

Time Dependent Tilt of a 20 m Deep Firn Pit

By H. Eisner, W. Ambach and H. Schneider*

Summary: On an approximately 20 m deep firn pit in the area of accumulation of a temperate Alpine glacier, tilting rates of the pit axis have been measured over a period of 11 years. During the first interval of the measuring period (from 1967 to 1974), the tilting rate does not show any disturbance due to the formation of crevasses. The share of the shear strain rate as well as of the longitudinal and vertical strain rates in the tilting rate of the pit axis is determined. Direct measurements of the longitudinal and vertical strain rates at the pit facilitate the calculation of the shear strain rate from the tilting rate of the pit axis. The values obtained in this manner may serve as a basis for the analysis of the rheological properties of the temperate firn.
During the second interval of the measuring period (from 1975 to 1978), a disturbance occurs due to the formation of a transverse crevasse, up to 4 m wide, 33.5 m on the upper side of the pit. In connection with the formation of the crevasse, the limiting value of the longitudinal strain rate for the tensile strength of the temperate firn is determined to be approximately $30.10^{-3}a^{-1}$.

Zusammenfassung: An einem etwa 20 m tiefen Firnschacht im Akkumulationsgebiet eines temperierten Alpengletschers wurden Neigungsänderungen der Schachtachse über eine Periode von 11 Jahren gemessen. Im ersten Intervall der Meßperiode (1967 bis 1974) verläuft die Neigungsänderung ohne Störung durch Spaltenbildung. Die Anteile der Scherverformungsrate, der longitudinalen und vertikalen Verformungsrate an der Neigungsänderung der Schachtachse werden ermittelt. Direkte Messungen der longitudinalen und der vertikalen Verformungsraten am Schacht ermöglichen die Berechnung der Scherverformungsrate aus der Neigungsänderung der Schachtachse. Die so ermittelten Werte der Scherverformungsrate können als Grundlage einer Analyse der rheologischen Eigenschaften des temperierten Firns dienen.
Im zweiten Intervall der Meßperiode (1975 bis 1978) tritt eine Störung der Bewegung durch Bildung einer bis zu 4 m breiten transversalen Spalte 33,5 m oberhalb des Schachtes auf. Der Grenzwert der longitudinalen Verformungsrate für die Zugfestigkeit des temperierten Firns wird im Zusammenhang mit der Spaltenbildung zu etwa $30.10^{-3}a^{-1}$ ermittelt.

1. INTRODUCTION

In order to investigate the rheological properties of the firn of a temperate Alpine glacier, deformation measurements were carried out on a firn pit form 1967 to 1978. Originally, the pit was 20 m deep, with a circular cross-section. In 14 different depths, 6 to 7 markers were placed at each level along the periphery of the wall and their relative distances were measured at yearly intervals. The deformed cross-sections of the pit were approximated by ellipses. The centres of these ellipses define the pit axis. The tilt of the pit axis is determined from the horizontal distances of the centres of the ellipses from the lead line and from their relative vertical distances.

The pit ist situated in the central region of the area of accumulation of Kesselwandferner (Ötztal Alps). The vertical density profile at the pit site is known, the values ranging from 631 kg/m³ to 864 kg/m³. The water equivalent of the mean annual net accumulation between 1967 and 1980 amounts to 1,3 m at this site. From velocity measurements on the surface it is known that longitudinal and transverse strain rates occur at the site of the pit (SCHNEIDER, 1970). With respect to the state of stress, therefore, the pit is not situated in a neutral zone.

First evaluations of the strain rates of the pit's deformation have been published already (EISNER & AMBACH, 1981; AMBACH & EISNER, 1983). In the present paper the shear strain rate is calculated from the time dependent tilt of the pit axis, under consideration of the longitudinal and vertical strain rates.

2. MEASUREMENT RESULTS

2.1 *General movement*

Geodetic measurements are expressed on a horizontal coordinate system, whereas a coordinate system,

* Dr. Heinrich Eisner, Institut für Experimentalphysik der Universität, Schöpfstraße 41, A-6020 Innsbruck
Prof. Dr. Walter Ambach, Institut für Medizinische Physik der Universität, Müllerstraße 44, A-6020 Innsbruck
Dr. Heralt Schneider, Institut für Mathematik der Universität, Innrain 52, A-6020 Innsbruck

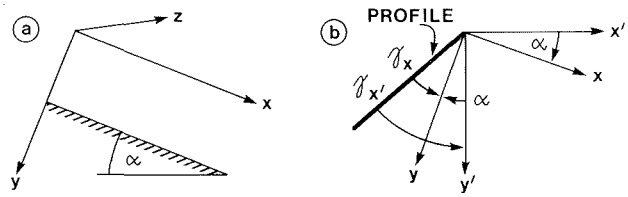

Fig. 1: Coordinate system applied.

Abb. 1: Verwendete Koordinationssysteme.

adjusted to the glacier surface and the flow direction, is applied for the evaluation of the strain rates (Fig. 1). Fig. 2 shows the positions of the pit and its flow line in relation to the surface. Due to the immersing movement, the bottom of the pit is lowered from a depth of 20 m to a depth of 34 m. From 1973 onwards, the bottommost level immerses into the water table, so that the water had to be pumped off for the surveying of the markers (AMBACH et al., 1978).

2.2 *Tilt of the pit axis*

Fig. 3a shows the time dependent horizontal displacements of the pit axis from the lead line. Initially, a slight tilt of the pit axis does already exist. With respect to the tilting rate of the pit axis, the measuring period can be subdivided into two intervals. From 1967 to 1974, an approximately uniform tilting rate of the pit axis is to be noted, whereas from 1975 onwards, a considerably higher tilting rate occurs in all depths. The tilting rate cannot, therefore, be assumed to be constant over the entire measuring period.

2.3 *Vertical strain rates of layer compression*

Contrary to the significant change in the tilting rate as from 1975 onwards, the vertical strain rates of the compression of layers remain approximately constant (Fig. 3b). Generally, layers situated in greater depths (No. 1 to No. 5) show a smaller vertical strain rate because of the higher density than layers closer to the surface (No. 6 to No. 13). Irregularities in the sequence of succession of the level occur because of the differences in structure due to inclusions of ice (Fig. 3b).

Fig. 4a shows the time dependent vertical displacements of the individual layers in relation to the bottommost layer. The distance between the topmost and the bottommost level decreases from 17,6 m to 11,9 m between 1967 and 1978; at the same time, the reference level (No. 1) is lowered by 13,7 m due to the immersing movement. In Fig. 4a as well, no sudden change in the vertical strain rate is noticeable which could be compared with the erratic change in the tilting rate of the pit axis around 1975.

2.4 *Longitudinal strain rates*

Fig. 5a shows the network of stakes, by means of which measurements of strain rates were carried out on the surface in the vicinity of the pit. Stakes L3 and L4 were reset at their original positions annually, stakes T1—T4 were left in their positions.

From Fig. 5b it can be noted that the longitudinal strain rate slightly increases with time, in accordance

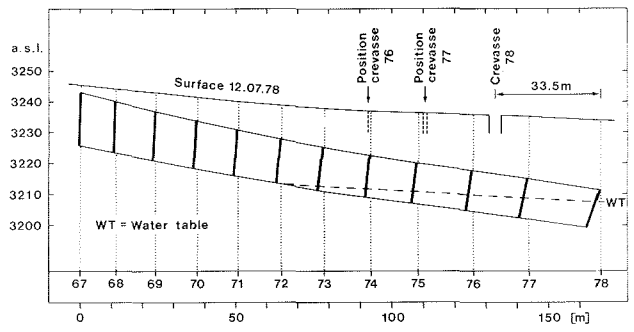

Fig. 2: Flow distance of pit from 1967 to 1978.

Abb. 2: Fließweg des Schachtes von 1967 bis 1978.

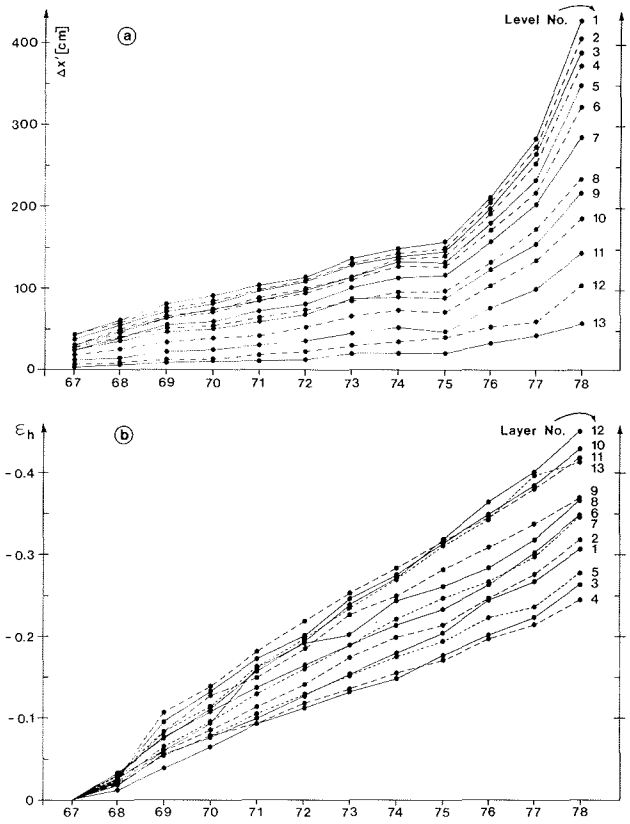

Fig. 3: a) Horizontal displacement of pit axis to the lead line (△x') as a function of time. The lead line is fixed in the centre of the ellipse of the topmost level (No. 14).
b) Strain of compression of individual layers ϵ_h as a function of time. Layer 1 is located between levels 1 and 2.

Abb. 3: a) Horizontale Distanzen der Schachtachse zum Lot (△x') als Zeitfunktion. Das Lot ist im Ellipsenmittelpunkt des obersten Niveaus (Nr. 14) fixiert.
b) Verformung der Schichtkompression ϵ_h als Zeitfunktion. Schicht 1 liegt zwischen Niveau 1 und 2.

with a general increase in velocity. In particular, it turns out that the longitudinal strain rate between L3-L4 and L3-pit takes an approximately parallel course up to 1975/76 (Fig. 5b, curve b, c). From this time onward, however, a strong increase in the strain rate L3-pit can be noted (curve b), caused by the formation of a crevasse (Fig. 2). The transverse strain rate in the pit area also shows a considerable change from 1975/76 onwards (curve d).

3. EVALUATION OF TILTING RATE OF PIT AXIS

3.1 *Tilt of pit axis*

Fig. 6 shows the tilt of the pit axis, taking the bottommost level (No. 1) as reference. The profiles were approximated by means of best fitting straight lines. The scatter of the measuring points around these lines is caused by great structural differences between the layers on the one hand. The layers of the balance years of 1964/65 and of 1965/66, for example, are annual accumulations of particularly great size and comparatively small density (Fig. 7). On the other hand, the bottommost layers immerse into the water table as from 1973 onwards, also presenting a systematic disturbance (AMBACH et al., 1978).

3.2 *Tilting rate and shear strain rate*

Calculation of the shear strain rate is made according to (PATERSON, 1981; RAYMOND, 1971)

$$\frac{\partial u}{\partial y} = \frac{\partial \gamma_x}{\partial t} - \gamma_x \left(\frac{\partial u}{\partial x} - \frac{\partial v}{\partial y}\right) + v \frac{\partial \gamma_x}{\partial y} - \gamma_z \frac{\partial u}{\partial z} \qquad (1)$$

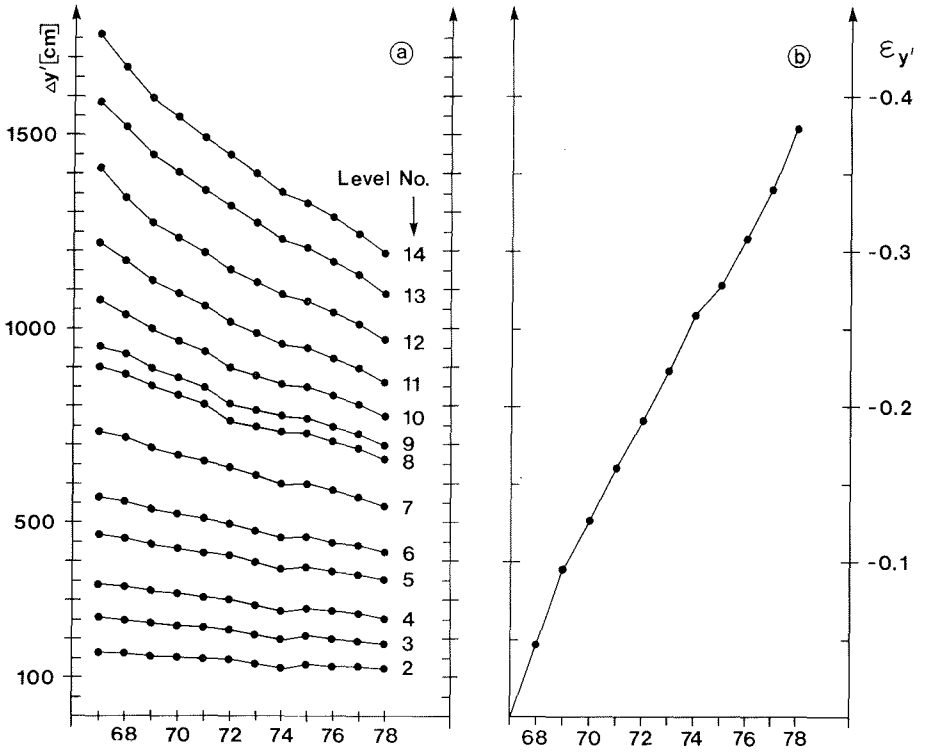

Fig. 4: a) Relative vertical displacement $\Delta y'$ of the individual levels as a function of time in relation to the bottommost level (No. 1).
b) Strain of compression $\epsilon_{y'}$ of the layer between level 1 and 14 as a function of time.

Abb. 4: a) Relative Vertikalabstände $\Delta y'$ der einzelnen Niveaus als Zeitfunktion bezogen auf das unterste Niveau (Nr. 1).
b) Verformung der Kompression $\epsilon_{y'}$ der Schicht zwischen Niveau 1 und 14 als Zeitfunktion.

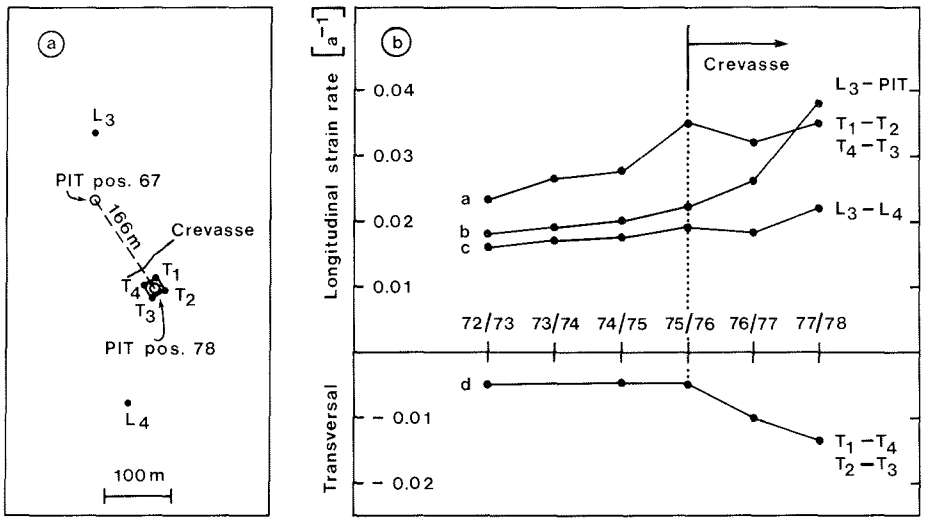

Fig. 5: a) Network of stakes for the measurement of the strain rates on the surface as well as position of the pit at the beginning and at the end of the measuring period.
b) Strain rates measured among various stakes and the pit.

Abb. 5: a) Pegelnetz zur Messung der Verformungsrate an der Oberfläche, sowie Lage des Schachtes zu Beginn und am Ende der Meßperiode.
b) gemessene Verformungsrate zwischen verschiedenen Pegeln und dem Schacht.

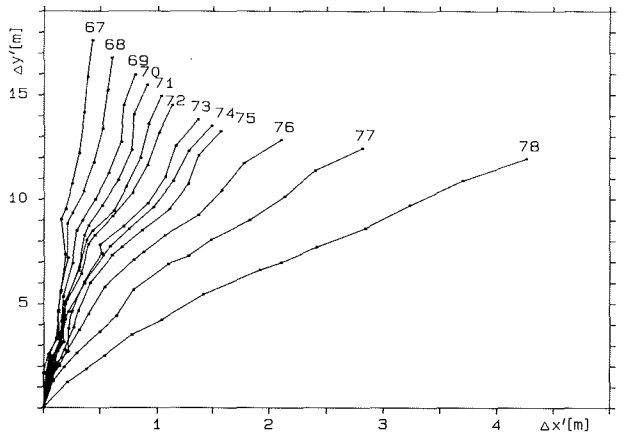

Fig. 6: Horizontal and vertical displacements ($\triangle x'$, $\triangle y'$) of the centres of the ellipses of the individual levels in relation to the bottommost level (No. 1) for the period from 1967 to 1978.

Abb. 6: Horizontal- und Vertikalabstände ($\triangle x'$, $\triangle y'$) der Ellipsenmittelpunke der einzelnen Niveaus bezogen auf das unterste Niveau (Nr. 1) für 1967 bis 1978.

moreover, it holds true that

$$\dot{e}_{xy} = \frac{1}{2}\left(\frac{\partial u}{\partial y} + \frac{\partial v}{\partial x}\right) \tag{2}$$

In this equation, u, v are the velocity components, $\gamma_X = \frac{dx}{dy}$ is the tilt of the pit axis in the x, y plane and γ_Z is the transverse tilt. All terms refer to the system x, y (Fig. 1). Because of the linear approximation of the tilt of the pit axis it is true that $\partial\gamma_X/\partial y = 0$. With $\gamma_Z = 0$ and

$$2r = \left(\frac{\partial u}{\partial x} - \frac{\partial v}{\partial y}\right) \tag{3}$$

equation 1 subsequently reads

$$\frac{\partial u}{\partial y} = \frac{\partial \gamma_X}{\partial t} - 2r\gamma_X \tag{4}$$

2r is a correction term relating to the longitudinal and the vertical strain rates. For positions where the pit axis is vertical to the surface, it holds true that $\gamma_X = 0$, thus equation 4 reads

$$\frac{\partial u}{\partial y} = \frac{\partial \gamma_X}{\partial t} \tag{5}$$

Fig. 8 shows the time dependent tilt of the pit axis represented as the slope of the best fitting straight line in the system x', y' (Fig. 1) and expressed in degrees. In addition, the respective slope of the surface along the flow line is inserted. In the point of intersection of both curves, the pit axis is vertical to the surface.

3.3 *Vertical position of the pit axis*

The tilt of the axis γ_x to the mean surface slope from 1967 to 1974 is represented in Fig. 9a. The measur-

---

a, b, c	coefficients of an approximation polynome	u, v, w	components of velocity
$\dot{e}_{xy}$	shear strain rate	x, y, z	coordinates (x parallel to surface)
r	parameter ($2r = \frac{\partial u}{\partial x} - \frac{\partial v}{\partial y}$)	x', y', z'	coordinates (x' horizontal)
t	time	α	surface slope
t_0	time of vertical position of pit axis to surface		
γ_x	tangent of angle of inclination of pit axis in x, y plane ($\gamma_X = dx/dy$)		
$\gamma_{x'}$	tangent of angle of inclination of pit axis in x', y' plane ($\gamma_{X'} = dx'/dy'$)		
γ_z	tangent of angle of inclination of pit axis in y, z plane ($\gamma_Z = dz/dy$)		
γ_0	γ_X for t = o		

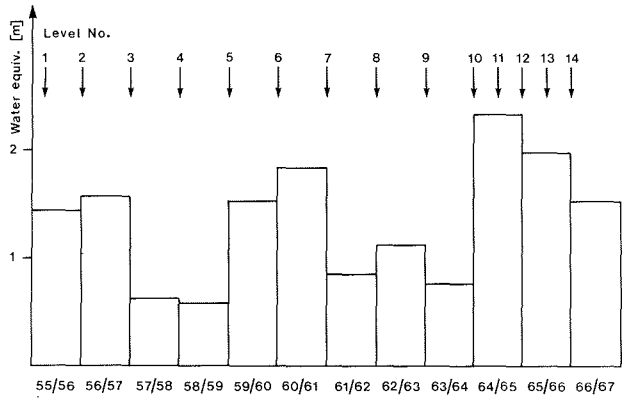

Fig. 7: Water equivalent of annual accumulations and positions of the individual levels.

Abb. 7: Wasseräquivalent der Jahresrücklagen und Positionen der Pegelniveaus.

ing points were approximated by the least square polynome

$$\gamma_x(t) = a + bt + ct^2 \tag{6}$$

The coefficients result in a = 0.0624, b = $-0.0109a^{-1}$, c = $-4.86.10^{-4}a^{-2}$. For positions where the pit axis is vertical to the surface, $\gamma_x = 0$ and thus it results

$$a + bt_o + ct_o^2 = 0 \tag{7}$$

with t_o = 4.74 a. This corresponds to a time between 1971 and 1972. The tilting rate of the pit axis for a position vertical to the surface can be obtained from equation 6 as

$$\left(\frac{\partial \gamma_x}{\partial t}\right)_{t_o} = b + 2ct_o \tag{8}$$

According to equations 5 and 2 and using the above mentioned values of b, c, t_o, we finally obtain

$$\frac{\partial u}{\partial y} = -15.5.10^{-3}a^{-1} \text{ und } \dot{e}_{xy} = -7.75.10^{-3}a^{-1} \tag{9}$$

By estimation the result is $\frac{\partial v}{\partial x} \sim 0.04 \frac{\partial u}{\partial y}$, so that $\frac{\partial v}{\partial x}$ can be neglected in equation 2, compared with $\frac{\partial u}{\partial y}$.

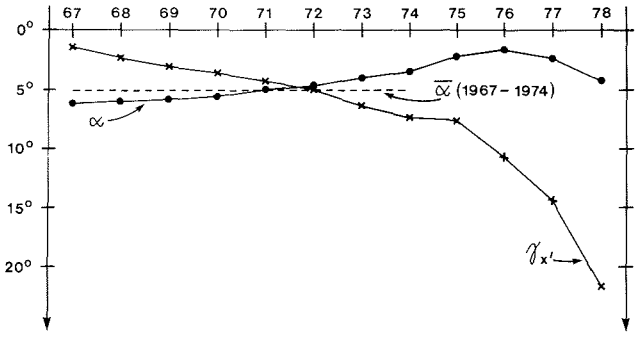

Fig. 8: Tilt of pit axis ($\gamma_{x'}$) in system x', y', and surface slope in the vicinity of the pit (α), as a function of time; mean value of surface slope between 1967 and 1974 ($\bar{\alpha}$), values converted into degrees.

Abb. 8: Neigung der Schachtachse ($\gamma_{x'}$) im System x', y' und Neigung der Oberfläche im Bereich des Schachtes (α), als Zeitfunktion; Mittelwert der Oberflächenneigung zwischen 1967 und 1974 ($\bar{\alpha}$). Werte in Grad umgerechnet.

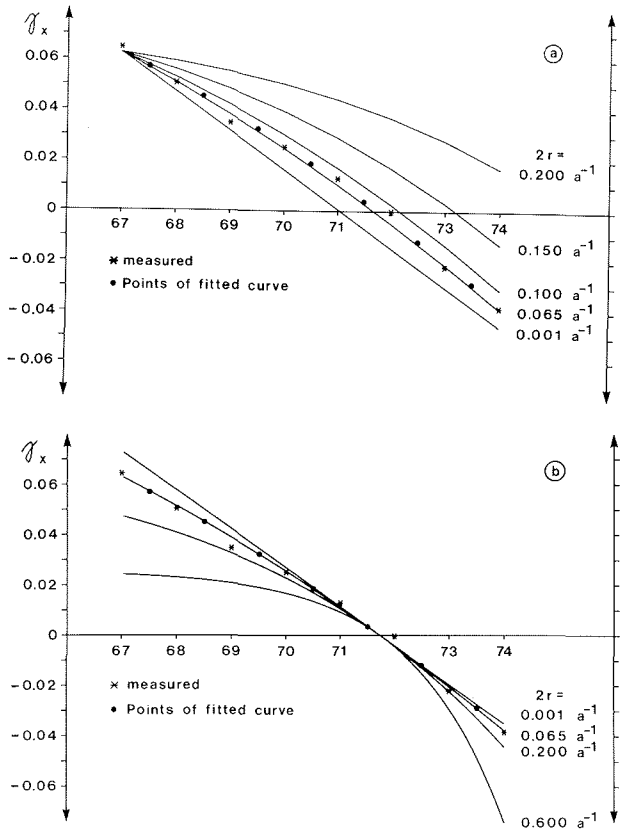

Fig. 9: a) Tilt of pit axis (γ_X) as a function of time in system x, y; (*) measuring points. Full circles are values according to equation 6; fully drawn curves are calculated as per equation 10 for fixed initial values of γ_X.
b) as a); fully drawn curves are calculated according to equation 10 for fixed point of intersection with time axis.

Abb. 9: a) Neigung der Schachtachse (γ_X) als Zeitfunktion im System x, y. * Meßpunkte; volle Kreise sind Werte nach Gl. 6. Durchgezogene Kurven sind nach Gl. 10 für festen Anfangswert von γ_X berechnet.
b) wie a); durchgezogene Kurven sind nach Gl. 10 für festen Schnittpunkt mit der Zeitachse berechnet.

4. RESULTS

4.1 *Period from 1967 to 1974*

From 1967 to 1974, no disturbance of the strain rates due to formation of a crevasse was noted so that the tilting rate measured can be used for the calculation of the strain rate.

In Fig. 9a, b, the temporary course of the pit's tilts measured $\gamma_x(t)$ is compared with the calculated values. For the conversion of the pit's tilt from system x', y' into system x, y, the mean surface slope for the evaluation period $\bar{\alpha} = 5.14°$ is applied (Fig. 8). Calculation of $\gamma_x(t)$ is carried out using the following steps:

— Solution of equation 4 for $\frac{\partial u}{\partial y}$ = constant and 2r = constant.
We get

$$\gamma_x(t) = \gamma_o e^{2rt} + \frac{1}{2r}\frac{\partial u}{\partial y}(e^{2rt} - 1) \qquad (10)$$

— Calculation of $\gamma_x(t)$ for various values of 2r according to equation 10. The following two methods of calculation were applied:
— $\partial u/\partial y = -15.5.10^{-3}a^{-1}$ (equation 9), $\gamma_o(1967) = 0.0624$ which are assumed to be constant values; $\gamma_o(1967)$ is identical with value "a" of equation 6; results see Fig. 9a.
— $\partial u/\partial y = -15.5.10^{-3}y^{-1}$ (equ. 9), $t_o = 4.74$ a (equ. 7) which are assumed to be constant values; for results see Fig. 9b.

In both cases, a good agreement of the course of the pit's tilt measured with the calculated values can be

obtained with $2r = 65.10^{-3}a^{-1}$.

From deformation measurements at the pit, 2r can be obtained directly and can be compared with the values calculated as follows: $\frac{\partial u}{\partial y}$ results from the deformation of the cross section of the pit due to longitudinal strain and is independent of the depth as $28.10^{-3}a^{-1}$ (EISNER & AMBACH, 1981). $\frac{\partial v}{\partial y}$ results from the vertical strain in the pit as $-36.10^{-3}a^{-1}$ (Fig. 4b). The value of $\frac{\partial v}{\partial y}$ was determined from Fig. 4b by the slope of the best fitting straight line. From direct measurements at the pit the value $2r = 64.10^{-3}a^{-1}$ results show good agreement with the calculated value $2r = 65.10^{-3}a^{-1}$ which was derived from Fig. 9a, 9b.

For the determination of 2r, constant mean values of the longitudinal and vertical strain rates were applied. From Fig. 5b, however, it can be seen that the longitudinal strain rate slightly increases with the time (curve a), whereas the amount of the vertical strain rate slightly decreases with the time. This decrease corresponds to the slight curvature of the curve in Fig. 4b. Increase and decrease do partly compensate each other, resulting in an approximately constant value for 2r.

4.2 *Period from 1975 to 1978*

Because of the formation of a transverse crevasse approximately 33,5 m on the upper side of the pit (Fig. 2 and 5), the tilting rate of the pit axis is disturbed from 1975 onwards and cannot be used for the calculation of the shear strain rate. If the evaluation for the period from 1975 to 1978 is carried out according to equation 10 as described in section 4.1, one does obtain a satisfactory agreement of the pit's tilts with the measured values with $\gamma_o(1975) = -0.0447$ and $2r = 480.10^{-3}a^{-1}$ (Fig. 10).

By doing so, $\frac{\partial u}{\partial y} = -15.5.10^{-3}a^{-1}$ was taken over from section 4.1. In Fig. 10, the disturbance of the movement due to the formation of a crevasse can clearly be noticed from the course of the measuring curve and from the erratic alteration of the value 2r >around 1975. For values of $2r > 65.10^{-3}a^{-1}$, the limiting value of the tensile strength of the firn is exceeded. According to equation 3, this corresponds to $\frac{\partial v}{\partial y} = -36.10^{-3}a^{-1}$ and to $\frac{\partial u}{\partial x} > 29.10^{-3}a^{-1}$. This results is in good agreement with the longitudinal strain rate in the pit area, measured immediately before the formation of the crevasse at the surface. From Fig. 5b (curve a), the measured longitudinal strain rate for the period 1974/75 results as $27.10^{-3}a^{-1}$, and for the period 1975/76 as $35.10^{-3}a^{-1}$, in accordance with the maximum value before the formation of the transverse crevasse $29.10^{-3}a^{-1}$ as calculated above.

5. FINAL REMARKS

If the movement is undisturbed by the formation of crevasses, the temporary course of the pit's tilt can be

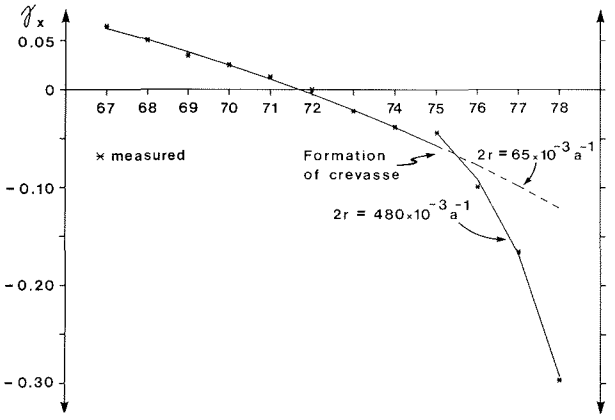

Fig. 10: Tilt of pit axis (γ_X) in system x, y as a function of time; (*) measuring points. Fully drawn curves calculated according to equation 10.

Abb. 10: Neigung der Schachtachse (γ_X) im System x, y als Zeitfunktion. * Meßpunkte; durchgezogene Kurven berechnet nach Gl. 10.

approximated in a satisfactory manner by equation 10. The influence of the longitudinal and vertical strain rates on the tilting rate has to be taken into consideration when calculating the shear strain rate. Only where the pit axis is vertical to the surface, the influence is nil.

The jerky alteration of the value 2r around 1975 from $65.10^{-3}a^{-1}$ to $480.10^{-3}a^{-1}$ is a consequence of the formation of the crevasse. This jerk develops when the crevasse opens due to an increased speed of the downhill edge of the crevasse after having exceeded the limit value for the tensile strength of the firn.

The value of the shear strain rate, obtained under consideration of the longitudinal and vertical strain rates, can be the basis for the determination of the rheological properties of the firn. A respective analysis is in preparation.

6. ACKNOWLEDGEMENT

The authors would like to express their gratitude to the Austrian Academy of Sciences (Akademie der Wissenschaften), Vienna, for the financial support; to the Federal Ministry for the Interior (Bundesministerium für Inneres), Vienna, for the transportation of material needed; and to all cooperators for the often exacting field works; as well as to Mr. K. Leitl for his cooperation in the evaluation of the measuring data.

References

Ambach, W. & H. Eisner (1983): Effective shear viscosity and effective bulk viscosity of firn of a temperate glacier (Kesselwandferner, Ötztal Alps, 1967—1978). — Ann. Glaciol. 4: 10—13.

Ambach, W., Blumthaler, M., Eisner, H., Kirchlechner, P., Schneider, H., Behrens, H., Moser, H., Oerter, H., Rauert, W. & H. Bergmann (1978): Untersuchungen der Wassertafel am Kesselwandferner (Ötztaler Alpen) an einem 30 Meter tiefen Firnschacht. — Z. Gletscherkde. Glazialgeol. 14 (1): 61—71.

Eisner, H. & W. Ambach (1981): Strain rate measurements in a 20 m deep firn pit in a temperate glacier (Kesselwandferner, Oetztal Alps, 1967—1978). — Z. Gletscherkde. Glazialgeol. 17 (2): 169—176.

Paterson, W. S. B. (1981): The physics of glaciers — Oxford.

Raymond, C. F. (1971): Determination of the three-dimensional velocity field in a glacier. — J. Glaciol. 10 (58): 39—43.

Schneider, H. (1970): Die Grundlagen der Vermessungen am Kesselwandferner (Ötztaler Alpen) und die Bewegung dieses Gletschers in den Haushaltsjahren 1965/66, 1966/67 und 1967/68. — Unpubl. thesis, Univ. of Innsbruck.